THE JOURNAL OF BIOLOGICAL CHEMISTRY VOL. 281, NO. 17, pp. 12187–12195, April 28, 2006

Vascular Endothelial Growth Factor (VEGF)/VEGF-C Mosaic Molecules Reveal Specificity Determinants and Feature Novel Receptor Binding Patterns*[S]

Received for publication, October 26, 2005, and in revised form, February 24, 2006 Published, JBC Papers in Press, February 27, 2006, DOI 10.1074/jbc.M511593200

Michael Jeltsch[‡], Terhi Karpanen[‡], Tomas Strandin[§], Kukka Aho[‡], Hilkka Lankinen[§], and Kari Alitalo[‡1]

From the [‡]Molecular/Cancer Biology Laboratory and Ludwig Institute for Cancer Research, Biomedicum Helsinki, Haartman Institute and Helsinki University Central Hospital, P.O. Box 63 (Haartmaninkatu 8), University of Helsinki and [§]Peptide and Protein Laboratory, Department of Virology, Haartman Institute and HUSLAB, P.O. Box 21 (Haartmaninkatu 3), University of Helsinki, Helsinki 00014, Finland

Vascular endothelial growth factors (VEGFs) and their receptors play key roles in angiogenesis and lymphangiogenesis. VEGF activates VEGF receptor-1 (VEGFR-1) and VEGFR-2, whereas VEGF-C activates VEGFR-2 and VEGFR-3. We have created a library of VEGF/VEGF-C mosaic molecules that contains factors with novel receptor binding profiles, notably proteins binding to all three VEGF receptors ("super-VEGFs"). The analyzed super-VEGFs show both angiogenic and lymphangiogenic effects *in vivo*, although weaker than the parental molecules. The composition of the VEGFR-3 binding molecules and scanning mutagenesis revealed determinants of receptor binding and specificity. VEGFR-2 and VEGFR-3 showed striking differences in their requirements for VEGF-C binding; extracellular domain 2 of VEGFR-2 was sufficient, whereas in VEGFR-3, both domains 1 and 2 were necessary.

The vascular endothelial growth factors (VEGFs)[2] are key molecules in the development and growth of blood and lymphatic vessels (1–3). Each VEGF is characterized by an individual receptor binding profile, which determines its scope of biological effects. For example, VEGF binds both VEGFR-1 and VEGFR-2 and is predominantly angiogenic, whereas VEGF-C binds VEGFR-2 and VEGFR-3 and promotes mainly lymphangiogenesis. The co-crystallization of placenta growth factor (PlGF) and VEGF with domain 2 of VEGFR-1 (4, 5) shows that a virtually identical set of residues in PlGF and VEGF form very similar receptor binding interfaces (5–7).

VEGF amino acid residues important for binding to VEGFR-2 have been identified by mutagenesis studies (7–9). However, it is unclear how receptor specificity is encoded within the VEGF family of growth factors. Furthermore, there are no structural data regarding VEGF-C interaction with its receptors. A mutant form of VEGF-C, which has lost its VEGFR-2 binding activity has been described, but the role of the mutated amino acid residue in receptor binding has not been analyzed (10).

Rational design of ligands often employs modification of their receptor binding profiles on the basis of structural data (11). Conversely, here we have deduced structural information from receptor binding data. To screen for structural elements of VEGF-C involved in specific receptor interactions, we created a library of mosaic molecules from VEGF and VEGF-C. Additional to the evaluation of individual residues based on the loss of ligand affinity upon mutation, we grafted VEGF-C segments into VEGF to gain VEGFR-3 binding. Because such DNA shuffling did not resolve the interaction determinants at the individual residue level, we scanned the regions that conferred VEGFR-3 binding by alanine mutagenesis to identify the residues that are important for specific receptor interaction. Finally, we showed *in vivo* that the introduction of additional receptor affinities into VEGF or VEGF-C modifies their biological effects, creating dual angiogenic/lymphangiogenic properties, which are somewhat weaker than the angiogenic and lymphangiogenic effects of VEGF and VEGF-C, respectively.

EXPERIMENTAL PROCEDURES

Creation and Screening of the VEGF/VEGF-C Mosaic Library—We maximized the identity of nucleotide sequences coding for the VEGF homology domain of VEGF and VEGF-C by silent mutagenesis (see the supplemental data). Two sets of nine DNA fragments coding for segments of VEGF and VEGF-C, respectively, were synthesized. The overhangs of these fragments corresponded to stretches of 100% nucleotide sequence identity between VEGF and VEGF-C. Two or three adjacent fragments were simultaneously ligated into a modified pKO Scrambler V912 vector (Stratagene, La Jolla, CA). Thus, four different vector sets were obtained (Fig. 1*B*). Two vector sets were then combined into 32 different vectors coding for the N-terminal halves of the mosaic molecules. Similarly, the two other vector sets were combined into 16 different vectors coding for the C-terminal halves. The final ligation created 512 different vectors. The expression plasmid pMosaic that hosted the library was constructed using sequences from pSecTagA and pICZα-A (both from Invitrogen), site-directed mutagenesis, and synthetic linkers. pMosaic contained a cytomegalovirus promoter, the immunoglobulin κ leader peptide for secretion, a C-terminal Myc epitope, and a hexahistidine tag for detection. The assembly of the library is schematically shown in Fig. 1*B*, and details can be found as supplemental data. All 512 constructs were separately transfected into 293T cells. After metabolic labeling with [^{35}S]methionine and [^{35}S]cysteine for 24 h, the conditioned medium was immunoprecipitated with anti-pentahistidine antibody (Qiagen, Valencia, CA) and VEGFR extracellular domain/immunoglobulin G Fc (VEGFR/IgGFc) fusion proteins. For the latter, the

* This study was supported by National Institutes of Health Grant 5 R01 HL075183-02 and the European Union Lymphangiogenomics Program (LSHG-CT-2004-503573LAG), the Novo Nordisk Foundation, the Finnish Technology Development Center, Aarne Koskelo Foundation, Farmos Foundation, Instrumentarium Science Foundation, Sigrid Jusélius Foundation, Finnish Cultural Foundation, Finnish Heart Research Foundation, and the Magnus Ehrnrooth Foundation. The costs of publication of this article were defrayed in part by the payment of page charges. This article must therefore be hereby marked "*advertisement*" in accordance with 18 U.S.C. Section 1734 solely to indicate this fact.

[S] The on-line version of this article (available at http://www.jbc.org) contains supplemental data.

[1] To whom correspondence should be addressed: Tel.: 358-9-19125511; Fax: 358-9-19125510; E-mail: kari.alitalo@helsinki.fi.

[2] The abbreviations used are: VEGF, vascular endothelial growth factor; VEGFR, VEGF receptor; αSMA, α smooth muscle actin; CAM, chorioallantoic membrane; PlGF, placenta growth factor.

Supplemental Material can be found at: http://www.jbc.org/cgi/content/full/M511593200/DC1

medium was supplemented with bovine serum albumin and heparin to final concentrations of 1% and 0.1 μg/ml. The protein A-bound fraction was analyzed in 15% SDS-polyacrylamide gels.

Construction of VEGFR/IgGFc Expression Vectors—To construct the VEGFR-2/IgGFc expression plasmid, the first three Ig homology domains of the extracellular part of VEGFR-2 were amplified by PCR using primers 5′-GCGGATCCTTGCCTAGTGTTTCTCTTGAC-3′ and 5′-CCAGTCACCTGCTCCGGATCTTCATGGACCCTGACA-AATG-3′ and cloned into the Signal pIgplus vector (Novagen, Madison, WI). The resulting plasmid was cut with BamHI and KpnI, treated with T4 polymerase, and ligated to itself. The expression plasmids for VEGFR-2/IgGFc and VEGFR-3/IgGFc (12) were transiently transfected into 293T cells, and the conditioned medium was used for the precipitation of growth factors. VEGFR-1/IgGFc was expressed in S2 cells and purified as previously described (12). The deletion series of the linker between VEGFR-3 domains 2 and 3 was created by PCR using the expression plasmid VEGFR-3/IgGFc as template, T7 as forward primer, and the following reverse primers: 5′-TCAGGATCCGCGAGCTCGT-TGCCTG-3′, 5′-TACAGGATCCCCTGTGATGTGCACCAG-3′, 5′-TCAGGATCCGCGTGCACCAGGAAGG-3′, and 5′-TCAGGATC-CGCGAAGGGGTTGGAAAG-3′.

The Ig homology domain 1 was deleted from the expression plasmid VEGFR-3/IgGFc by site-directed mutagenesis using primers 5′-CCTT-GAACATCACGGAGGAGTCACACGTCAGAGACTTTGAGCAG-CCATTCATCAACAAGC-3′ and 5′-AGCTGCTGGTAGGGGAGA-AGGATCCTGAACTGCACCGTGTGG-3′ and excision of the BamHI fragment from the resulting plasmid. The plasmid coding for VEGFR-3 domains 2 and 3 was constructed by transfer of the SphI fragment from the original expression plasmid VEGFR-3/IgGFc into the plasmid encoding only VEGFR-3 domain 2. The sequences encoding four different versions of domain 2 of VEGFR-2 were amplified using forward primer 5′-AGCGCTAGCGTTCAAGATTACAGATCTC-C-3′ and reverse primers 5′-CTAGGATCCCCTACAACGACAACT-ATG-3′, 5′-CTAGGATCCACATCATAAATCCTATAC-3′, 5′-GCA-TGGTCTCGGATCATGAGACGGACTCAGAAC-3′, and 5′-CTAG-GATCCTTTTCTCCAACAGATAG-3′; subsequently the NheI- and BamHI- or BsaI-cut PCR products were subcloned into NheI and BamHI-cut Signal pIgplus vector.

VEGFR Phosphorylation, Bioassay, and Determination of Relative Affinities Using Enzyme-linked Immunosorbent Assay—Receptor phosphorylation was analyzed in porcine aortic endothelial VEGFR-2 (13) and porcine aortic endothelial VEGFR-3 cells (14), as described previously (15), using purified growth factors at concentrations of 20 nM. The bioassays using stably transfected Ba/F3 cells have also been described previously (16–19). To determine the relative affinities of the VEGF/VEGF-C mosaics, serial dilutions of competing $VEGF_{165}$ or ΔNΔC-VEGF-C and VEGFR/IgGFc were added in a subsaturating 1:15 molar ratio to MaxiSorp microtiter plates (Nunc, Naperville, IL) coated with 400 ng of purified growth factor. After 16 h, the receptors bound to the plate were quantified using biotinylated mouse anti-human IgGFc and streptavidin-alkaline phosphatase (both from Zymed Laboratories Inc., San Francisco, CA), and the competitor concentration that resulted in half-maximal binding of VEGFR/IgGFc to mosaic molecules was determined (EC_{50}, absolute values given in the supplemental data).

Surface Plasmon Resonance Analysis—Binding of VEGF-C and its mutants to VEGFR-1, -2, and -3 were analyzed with surface plasmon resonance in the Biacore 2000™ biosensor (Uppsala, Sweden). Flow cells of a CM5 biosensor chip were covalently coated with VEGFR/IgGFc fusion proteins via standard amine coupling. The binding of the alanine scan mutants was then analyzed in the standard Biacore running buffer (10 mM Hepes, pH 7.4, 150 mM sodium chloride, 3 mM EDTA, 0.005% surfactant P-20) following the instructions of the manufacturer. The kinetics of the VEGF-C interaction with VEGFR-2 and -3 were determined at varying concentrations of VEGF-C (20–300 nM) over a surface to which 1500 resonance units of the respective receptor had been coupled. The VEGFR-2 and -3-immobilized flow cells were regenerated after every injection with a pulse of 100 or 20 mM hydrochloric acid, respectively. The coupling level used in the screening experiments of the interactions was chosen to be 6000 resonance units for VEGFR-2, and the concentration of VEGF-C mutants was 1 μM. The coupling level of the more reusable VEGFR-3 surface was kept at 1500 resonance units, and the concentration for screening of mutants was chosen to be 100 nM. Replicative screening experiments were done on freshly coupled surfaces. The coupling levels of the receptors and the concentrations of the mutants varied between the experiments. The contact time of VEGF-C and its mutants was 5 min and the flow rate 20 μl/min. The data were evaluated by first subtracting the sensorgram obtained from the empty control flow cell from the sensorgrams of the flow cells containing VEGFR-2 or -3. The obtained curves were fitted to the natural logarithmic 1:1 Langmuir binding model of the BiaEvaluation 3.1 software package (Biacore) to obtain the relative binding levels and the relative dissociation constants of the mutated VEGF-C proteins.

Protein Production, Purification, and Gel Filtration—Ten selected mosaic VEGFs were produced in insect cells using the Bac-to-Bac system. Sf9 and High Five cells were maintained in Sf900II (all Invitrogen) according to the instructions of the supplier. First, the coding sequences for the melittin signal peptide and a hexahistidine tag were inserted into the transfer vector pFASTBAC1 as described previously (20), and subsequently, the coding sequences of the VEGF/VEGF-C mosaic molecules were subcloned into this construct. Details about the growth factors and control proteins are listed in the supplemental data. To produce the proteins for the VEGFR-1 bioassay, the conditioned medium of the baculovirus-infected High Five cells was concentrated 50-fold using Centricon C-10 spin columns (Millipore, Bedford, MA) diluted into Dulbecco's modified Eagle's medium, and the concentration of the mosaic molecules was determined by densitometry.

To purify protein for the chorioallantoic membrane (CAM) assay, conditioned medium of High Five cells was harvested 72 h after infection and dialyzed against 30 mM sodium phosphate and 400 mM sodium chloride, pH 6. The pH was adjusted to 8.0, and Ni^{2+}-nitrilotriacetic acid Superflow resin (Qiagen) was added. The samples were agitated for 12 h at +4 °C. The resin was then collected and applied to the chromatography columns. The columns were washed with 30 mM sodium phosphate, 400 mM sodium chloride, 600 mM glycerol, and 20 mM imidazole at pH 8.0, and the bound proteins were eluted with imidazole, dialyzed against 0.1% trifluoroacetic acid, and sterilized using Millex-GV filters (Millipore). The proteins were checked in silver-stained 15% polyacrylamide gels and quantified using the BCA protein assay kit (Pierce).

Coding sequences for the alanine scan mutants used in the surface plasmon resonance analysis and the VEGFR-2/VEGFR-3 bioassays were generated by site-directed mutagenesis using megaprime-based PCR mutagenesis or the QuikChange method (Stratagene). Coding sequences were then subcloned into the pMT-BiP/V5HisC vector (Invitrogen) for expression in insect cells. Protein from 50 ml of HyQ Sfx insect medium (Hyclone, Logan, UT) conditioned for 5 days by stably expressing S2 cells was purified by Ni^{2+}-nitrilotriacetic acid affinity chromatography as described above followed by buffer exchange against standard Biacore running buffer using a HR10/10 Fast Desalting column on an Äkta Explorer (GE Healthcare, Chalfont St. Giles, UK).

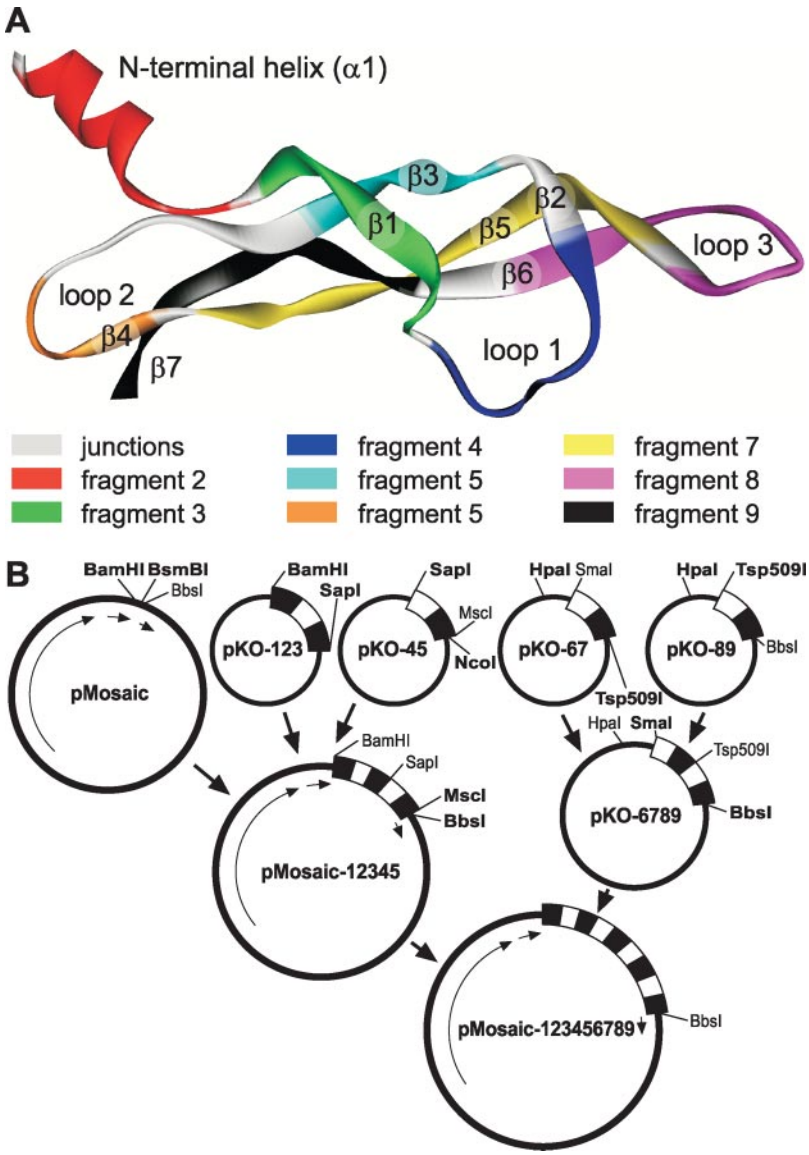

FIGURE 1. **Construction of the cDNA expression library and fragment structure of the mosaic molecules.** *A*, fragmentation of polypeptide segments are shown on a *ribbon model* of the VEGF subunit. The nucleotide sequences corresponding to individual segments are given as supplemental data. *B*, VEGF/VEGF-C mosaic molecules were assembled from four sets of vectors in two cloning steps, as shown. Sequences coding for VEGF and VEGF-C fragments are shown in *white* or *black*. Restriction sites used for cloning are shown in *bold*. *Arrows within the plasmid circles* indicate the locations of the cytomegalovirus promoter, the immunoglobulin κ signal peptide, and the histidine tag.

Gel filtration was performed on a Superdex 75 10/300 GL column (GE Healthcare) calibrated with a gel filtration low molecular weight calibration kit (GE Healthcare) using phosphate-buffered saline as eluent, a flow rate of 0.75 ml/min, and a sample volume of 200 μl. Analysis was performed using the Unicorn 4.1 software package (GE Healthcare).

CAM Assay—The CAM assay was carried out as described previously (21). Disks punched from Thermanox coverslips (Nunc) with the sterile salt- and carrier-free protein were applied to day 13 CAM, and after 3 days, the specimens were either fixed in 4% paraformaldehyde or 0.5% ZnCl and embedded into paraffin or embedded into TissueTek and subsequently frozen. Specimens were photographed in an Olympus SZX9 stereomicroscope. Carrier disks alone and human serum albumin were used as negative controls. Quantitation of angiogenesis in the transparent CAM was based on the optical density of the digitized microphotographs using computer-assisted image analysis (22). Mean relative optical density was measured from vessels with a diameter <0.1 mm using the program ImageJ (23). Lymphangiogenesis was quantitated from four 1125-μm view fields from hematoxylin and eosin-stained CAM sections located at the rim of the application disks. The ratio between the area occupied by lymphatic spaces and the total area was determined using ImageJ (23).

Immunohistochemistry—Immunohistochemistry was performed on sections of CAMs treated with 2.5 μg (control proteins) or 25 μg (mosaic proteins) of growth factor. Antiserum against Prox-1 was raised in rabbits (24); the protein A-bound fraction was used for the staining of unfixed frozen sections. Anti-α-smooth muscle actin (anti-αSMA) antibody (Sigma) was used at a dilution of 1:100, and the von Willebrand Factor antiserum (DAKO, Glostrup, Denmark) at a 1:300 dilution was used for the paraffin sections or at 1:500 on frozen sections.

RESULTS

Mosaic VEGFs with Novel Receptor Binding Profiles—Based on eight hot spots of sequence homology at the nucleotide level (supplemental data), we fragmented the VEGF homology domains of VEGF and VEGF-C into nine subunits and swapped the homologous fragments in all combinations (Fig. 1). All clones were transiently expressed in 293T cells, and the factors were precipitated from the conditioned medium of metabolically labeled cells using soluble VEGFR/IgGFc fusion proteins. To our surprise, the library contained molecules with all possible recep-

TABLE 1
Receptor binding frequencies among mosaic VEGFs

Receptor binding profile	*n*
VEGFR-1 and VEGFR-2	26
VEGFR-2 and VEGFR-3	28
VEGFR-1	25
VEGFR-2	25
VEGFR-3	26
VEGFR-1 and VEGFR-3	3
All three VEGF receptors	10
None	255
Not expressed or not secreted	114
Total	512

tor binding combinations (summarized in Table 1), including 10 factors binding to all three VEGF receptors (called here "super-VEGFs"). On the other hand, most of the molecules containing VEGF-derived fragment 3 and VEGF-C-derived fragment 7 were not secreted by the transfected cells (supplemental data).

Composition of the Mosaic Molecules—The apparent molecular masses of the dominant polypeptide species (19 or 21 kDa) were 4 or 6 kDa higher than predicted from the amino acid sequence. A comparison of the mobilities of the recombinant proteins shown in Fig. 2*A* and the schematic structures shown in Fig. 2*E* indicate that the reason for the size difference is the utilization of the *N*-linked glycosylation sites in fragments 7 (both VEGF and VEGF-C) and 9 (VEGF-C). Enzymatic deglycosylation and analysis of glycosylation-deficient mutants of VEGF-C confirmed that VEGF-C indeed uses both potential N-glycosylation sites (supplemental data). The compositions, apparent molecular masses, and receptor binding profiles of 10 mosaic molecules that were selected for further analysis are described in Fig. 2*E*.

The pattern of receptor interaction correlated with the composition of the mosaic molecules. VEGF-derived fragments 2 and 7 were required for VEGFR-1 binding, as none of the molecules with these fragments derived from VEGF-C could bind VEGFR-1. However, many mosaic molecules containing VEGF-derived fragments 2 and 7 bound efficiently to VEGFR-2 and -3; thus, these fragments were classified as "promiscuous." Also, fragment 3 of VEGF favored VEGFR-1 binding. Although required, fragments 2, 3, and 7 alone were not sufficient for VEGFR-1 binding.

VEGFR-3 Specificity and Binding Determinants—Unlike the binding to VEGFR-1, which depended strictly on VEGF-derived fragments 2 and 7, no single fragment of VEGF-C was absolutely required for binding to VEGFR-3. However, a bias toward VEGF-C-derived fragments was observed in the presumed bottom face of the molecule (fragments 4, 5, and 8). A predominantly VEGF-derived bottom face of the molecule precluded VEGFR-3 binding. Of the 67 VEGFR-3 binding molecules, 52, 56, and 45 had VEGF-C-derived fragments 4, 5, and 8, respectively. The importance of VEGF-C-derived fragments 4 and 8 for VEGFR-3 binding is exemplified in mosaic molecule 14–9, where these two fragments alone are sufficient to introduce VEGFR-3 binding into VEGF. Analogous to the promiscuous VEGF-derived fragments 2 and 7, the presence of VEGF-C-derived fragments 4, 5, and 8 did not inhibit VEGFR-1 or -2 binding.

Identification of Critical Residues by a Mutagenesis Scan of VEGF-C—To determine how individual amino acid residues within fragments 4, 5, and 8 were contributing to receptor binding, we mutated the non-conserved residues in these fragments into alanine residues to evaluate their effects on VEGFR-3 and -2 binding by surface plasmon resonance analysis (Fig. 3).

Only a few single amino acid mutants showed a pronounced increase in the apparent K_d for VEGFR-3, with the Cys^{156}→Ala mutation being most efficient in reducing both VEGFR-2 and -3 binding. When the same cysteine residue was mutated into a serine residue, only VEGFR-2

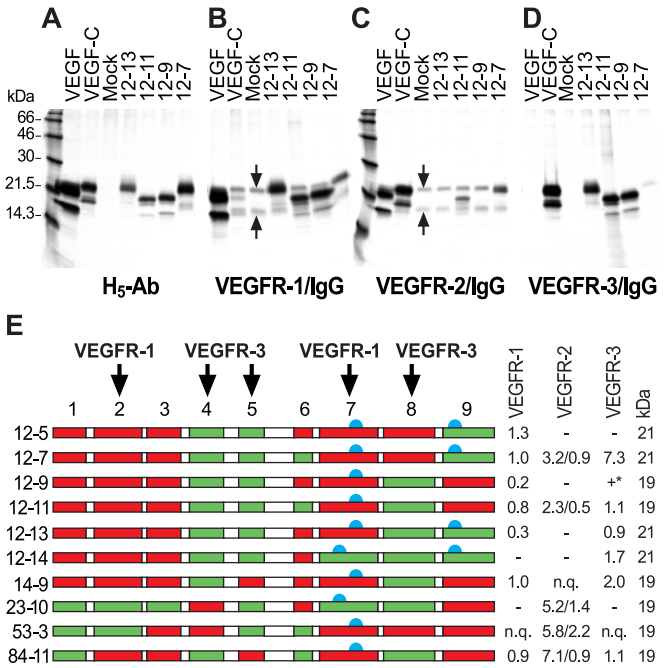

FIGURE 2. **The segment composition, molecular masses, and receptor binding properties of 10 mosaic molecules.** *A–D*, conditioned medium from transfected and metabolically labeled 293T cells was precipitated with the indicated VEGFR/IgGFc fusion proteins or the anti-histidine tag antibody. Note that VEGFR-1/IgGFc and VEGFR-2/IgGFc precipitate also endogenous VEGF (*arrows* in the *Mock* lanes of *B* and *C*). *E*, *red segments*, VEGF sequence; *green segments*, VEGF-C sequence; *white segments*, stretches of identity used in the construction of the library. The *arrows* indicate fragments containing receptor specificity determinants. *Blue dots* mark the glycosylation sites. Relative affinities are given as EC_{50} parent molecule/EC_{50} mosaic molecule. VEGFR-2 affinities relative to both $VEGF_{109}$ (*left*) and VEGF-C_{109} (*right*) were determined; numbers >1 indicate reduced binding affinity. A *minus sign* indicates no detectable interaction. The supplemental data provide a complete list of all 512 mosaic molecules and their receptor binding profiles. *, relative affinity was not determined; *n.q.*, not quantified due to low signal level; *Ab*, antibody.

binding was compromised, with VEGFR-3 binding remaining largely unaffected. To determine the cause of this difference, we used gel filtration to check the dimerization status of these mutants. For the Cys^{156}→Ala mutant, the molar ratio of monomeric to dimeric molecules was 4.6 to 1. However, this can only partially explain the difference, because the Cys^{156}→Ser mutant also showed a significant monomeric component with a molar ratio of 2 to 1. In fragments 4 and 8, the highest increase in the apparent K_d for VEGFR-3 binding was observed upon mutation of Phe^{151} and Pro^{198} residues, respectively.

We confirmed that the increase of apparent K_d and the reduction in total binding translated into reduced signaling using a cell growth/survival bioassay in Ba/F3 cells expressing a chimeric VEGFR-3EC/Epo or VEGFR-2EC/Epo receptor (Fig. 3). For several mutants, notably the double deletion of Leu^{192} and Ser^{193}, the reduction of activity in the bioassay was higher than expected when compared with other mutants whose apparent K_d and binding level were altered to a similar degree. A marked exception was the Pro^{198}→Ala mutant of VEGF-C; its complex with VEGFR-3 appeared to be very unstable. However, neither total ligand binding nor survival signaling in the Ba/F3 assay were significantly affected.

The Minimal VEGF-C Binding Fragment of VEGFR-3 and VEGFR-2—The extent of the extracellular domain necessary for VEGF binding differs between VEGFR-1 and VEGFR-2. The second extracellular Ig homology domain of VEGFR-1 alone is sufficient for VEGF binding, whereas VEGFR-2 also requires the presence of the third domain. Moreover, the exact amount of linker between domains 2 and 3 of VEGFR-1 determines whether a specific domain

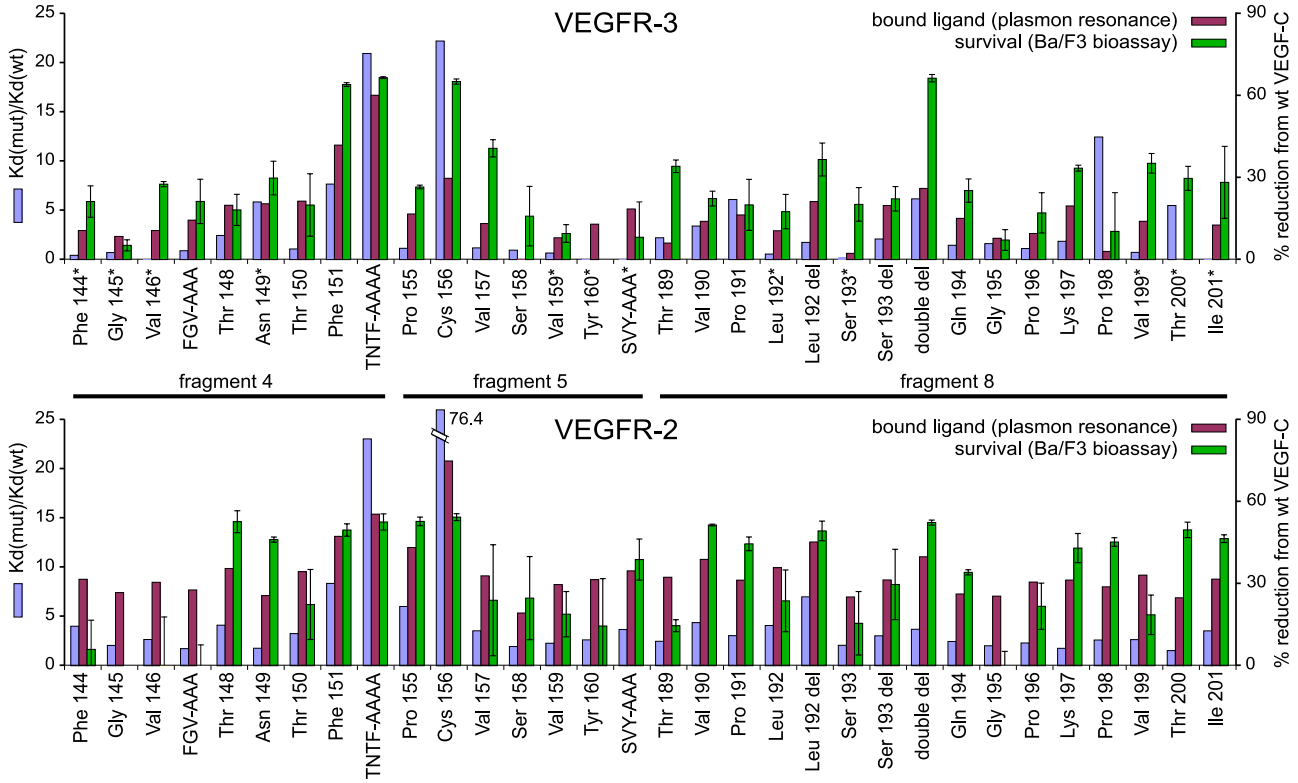

FIGURE 3. **Representative screens for receptor binding of VEGF-C mutants and Ba/F3 bioassays.** Apparent dissociation constant (K_d), binding level impairments, and reduction of the survival-promoting ability were used to qualify mutations. For several mutants, the ratio of the apparent K_d values for VEGFR-3 binding could not be calculated with confidence because of variation between replicative experiments; these residues are marked with an *asterisk*. *mut*, mutant; *wt*, wild type; *del*, deletion; FGV-AAA, TNTF-AAAA, and SVY-AAA denote compound mutants.

2-only construct can bind VEGF (4). To determine how much of the linker between the corresponding domains of VEGFR-2 and -3 is necessary for VEGF-C binding, we created a series of successive receptor deletion mutants. VEGF-C bound efficiently to soluble fusion proteins containing domains 1 and 2 of VEGFR-3 plus the linker between domains 2 and 3 up to Gly^{226} (supplemental data). When three additional residues were deleted, the fusion protein failed to be expressed. Thus, the minimal VEGF-C binding fragment of VEGFR-3 appears to extend C-terminally approximately to the same boundary as the minimal VEGF binding fragment of VEGFR-1. Although domain 2 of VEGFR-1 is sufficient for VEGF binding (4), no binding of VEGF-C occurred to VEGFR-3/IgGFc fusion proteins consisting of only domain 2 (including various lengths of the linker) or domains 2 and 3 (supplemental data). In contrast, VEGF-C bound efficiently to the second domain of VEGFR-2 consisting of residues 118–220; constructs containing an additional 6 or 12 C-terminal residues showed reduced interaction (supplemental data).

Mosaic VEGFs Induce VEGFR-2 and -3 Phosphorylation—To confirm the binding data, we assayed the dimerization-induced autophosphorylation of native VEGF receptors. For the phosphorylation assay, we chose a growth factor concentration that would saturate the response to VEGF and VEGF-C but allow the detection of differences in less active molecules. The mosaic factors 12–11, 84–11, and 12–14 were almost as potent as VEGF-C in inducing the phosphorylation of VEGFR-3 (Fig. 4*A*). Many of the mosaic molecules, however, induced a weaker VEGFR-2 phosphorylation than VEGF or VEGF-C (Fig. 4*A*). The receptor phosphorylation data mirrored the receptor binding data, with the exception of molecule 12–14. This mosaic factor induced VEGFR-2 phosphorylation but did not precipitate with the soluble VEGFR-2/IgGFc protein for reasons yet to be determined. As VEGFR-1 activation cannot be measured in terms of receptor phosphorylation (25, 26), we used a bioassay to demonstrate biological activity (Fig. 4*B*). All VEGFR-1 binding mosaic molecules were able to mediate survival of the stably transfected chimeric VEGFR-1EC/Epo receptor Ba/F3 cells, some at similar concentrations to VEGF. Mosaic molecules that were negative in the VEGFR-1 binding screen showed residual activity at very high concentrations.

Mosaic VEGFs Are Angiogenic and Lymphangiogenic—To simultaneously analyze the angiogenic and lymphangiogenic potential of the mosaic molecules *in vivo*, the purified proteins were applied to differentiated chick CAM (Fig. 5) (21). After incubation for 3 days, the blood vessels of the CAM were identified by staining for αSMA and von Willebrand factor, whereas the transcription factor Prox-1 was stained to identify the lymphatic vessels (Fig. 6*A*).

The mosaic VEGFs that bound to VEGFR-2 gave an angiogenic response in the CAM (Fig. 5). Similarly, a lymphangiogenic response was obtained with all tested mosaic VEGFs that showed significant binding to VEGFR-3. However, the effects of the mosaic VEGFs on the CAM were weaker than those of either parental molecule; to achieve comparable effects, 5–10-fold more protein had to be applied. The angiogenic control protein $VEGF_{109}$ and the lymphangiogenic control protein $VEGF\text{-}C_{109}$, which comprised exactly the same minimal receptor binding domain as the mosaic molecules, also showed reduced potency when compared with native $VEGF_{165}$ and mature VEGF-C, respectively. Of the two super-VEGFs tested, 12–11 was mostly angiogenic, with only a minor lymphangiogenic effect (Fig. 5*B*), and 84–11 was mostly lymphangiogenic, with only minor angiogenic activity (Fig. 5*B*).

Because the effects of the monospecific mosaic VEGFs were moderately weak in the CAM assay, we expressed and assayed for comparison

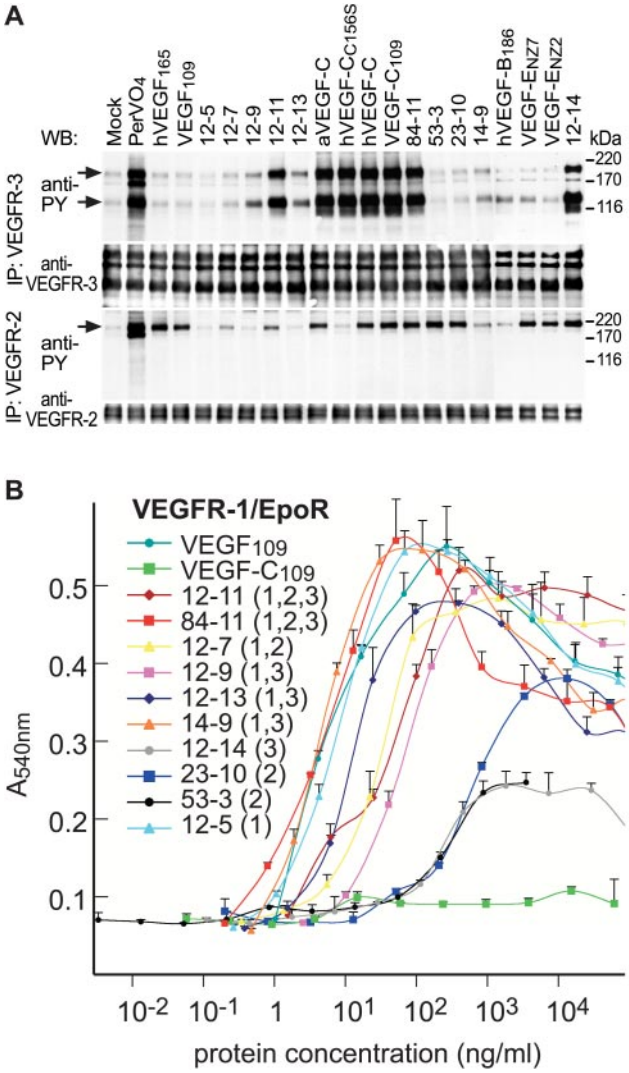

FIGURE 4. **VEGFR-1EC/Epo receptor activation and stimulation of receptor phosphorylation by the purified mosaic molecules.** *A*, immunoprecipitation (*IP*) with VEGFR-3 (14)- and VEGFR-2 (50)-specific antiserum and Western blotting (*WB*) with phosphotyrosine (*PY*)-specific antibody 4G10 (Upstate Biotechnology, Charlottesville, VA) from porcine aortic endothelial cells after a 5-min stimulation with the indicated ligands; *PerVO*$_4$ denotes the tyrosine phosphatase inhibitor pervanadate. After the detection of phosphotyrosine residues, the blots were stripped and reprobed with receptor-specific antibodies (14, 50) to verify loading of equal protein amounts. *Arrows* indicate phosphorylated receptor bands. *B*, the growth of VEGFR-1EC/Epo receptor chimera-expressing Ba/F3 cells is shown in optical density units of the non-radioactive cell proliferation assay as a function of the concentration of mosaic molecules in the growth medium. Molecules 23–10, 53–3, and 12–14, which could not be precipitated with soluble VEGFR-1/IgGFc fusion proteins showed 100–1000-fold reduced activity, and only VEGF-C was completely inactive in the assay. The *numbers in parentheses* in the legend indicate which VEGF receptors each individual mosaic molecule binds.

VEGF family members VEGF-B$_{186}$ (27), VEGF-E (28, 29), and the Cys^{156}→Ser mutant of VEGF-C (10). VEGF-E and the mosaic factor 53–3, which bind only VEGFR-2 were equally angiogenic on the CAM, but weaker than the factors that bound to both VEGFR-1 and -2 (data not shown). Compared with VEGF-C, the Cys^{156}→Ser mutant of VEGF-C induced a somewhat weaker lymphangiogenic response. VEGF-B$_{186}$ was without effect in the CAM.

DISCUSSION

Three ligands and two ligand-receptor complexes have been crystallized in the VEGF/VEGFR family, yet the mechanisms of receptor specificity determination are not clear. To pinpoint the determinants of receptor specificity in VEGF-C *versus* VEGF, we shuffled their coding

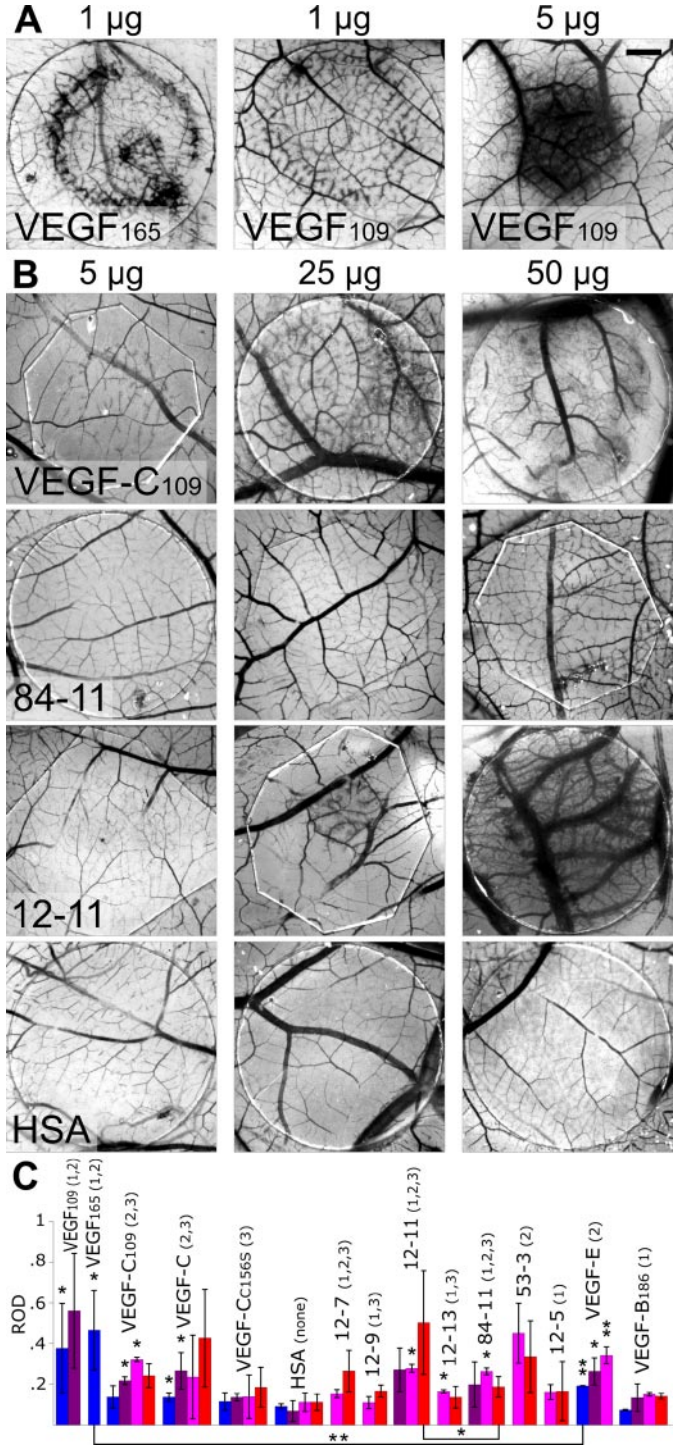

FIGURE 5. *A* and *B*, angiogenic effects of the mosaic molecules in the chick CAM. Different amounts of the recombinant mosaic proteins were dried on coverslips and applied to the 13-day CAM for 3 days. Note that the area of highest growth factor concentration and the strongest angiogenic response forms an *uneven circle* near the rim. The lymphatic vessels are inconspicuous. Occasionally, however, the huge lymphatic sinuses observed after the application of excess amounts of VEGF-C were filled with blood (data not shown). *Scale bar*, 1 mm. *C*, quantitation of angiogenesis by densitometry measuring the mean relative optical density (*ROD*) in the application area. Applied protein amounts are color-coded *blue* (1 μg), *magenta* (5 μg), *pink* (25 μg), and *red* (50 μg). For VEGF$_{109}$, VEGF$_{165}$, and VEGF-E, higher doses than shown here were mostly lethal to the embryo. *Numbers in parentheses* indicate which VEGF receptors the growth factor binds. Statistically significant results (Student's *t* test with H0, human serum albumin = sample) are indicated *above* the *error bars*, and the two sample *z* statistics for comparisons relevant to the discussion are given below the *x*-axis. * and ** denote *p* values of <5 and <1%, respectively. *HSA*, human serum albumin.

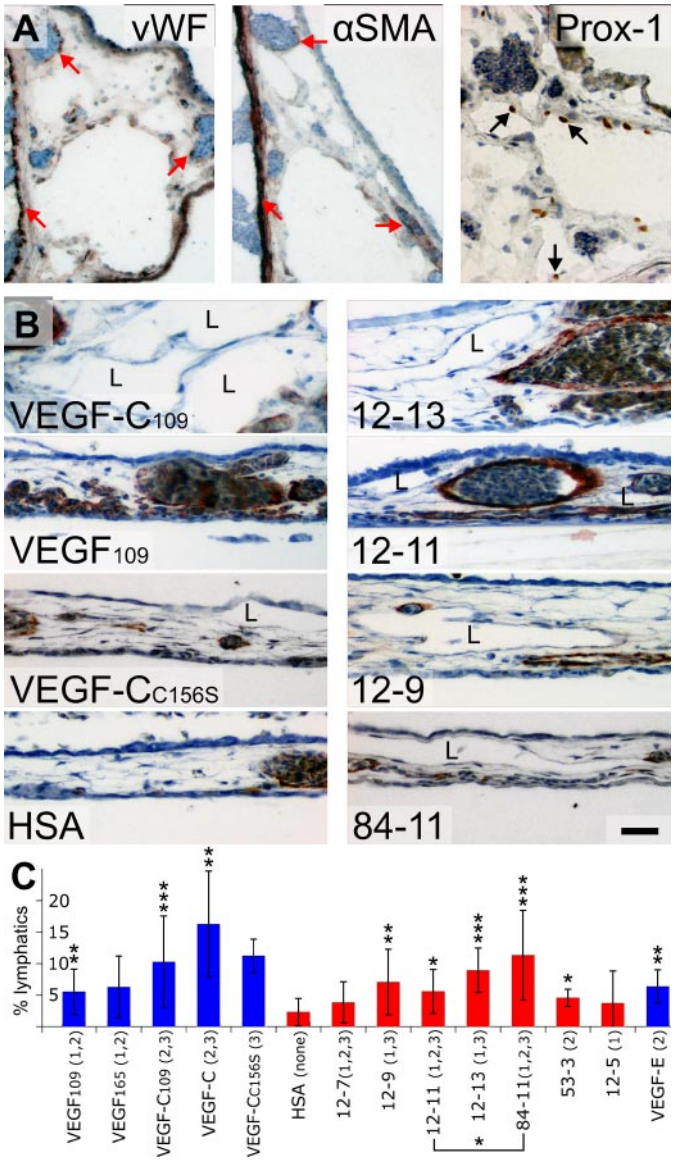

FIGURE 6. **Characterization of the vasculature of the chick CAM treated with recombinant VEGF, VEGF-C and mosaic growth factors.** *A*, in frozen serial sections, antibodies against αSMA stained all large blood vessels (*red arrows*). The CAM lymph vessels are devoid of smooth muscle, except for the largest collectors in the allantoic stalk (21). Antibodies against the von Willebrand factor (*vWF*) bound only to blood vessels and the largest lymph vessels in the CAM but not the lymph capillaries (*L*). The lymphatic nature of the αSMA- and von Willebrand factor-negative vessels was confirmed using the Prox-1 marker (*black arrows*) (51). *B*, αSMA staining of the CAM specimens. In CAMs treated with VEGF-C_{109} or the mosaic factors 84–11 and 12–9, the area of application was covered by a large lymphatic plexus. ΔNΔC-VEGF-C_{C156S} and 12–13 were moderately lymphangiogenic, whereas mosaic factor 12–11 was weakly lymphangiogenic. In comparison, very few lymph vessels were detected in HSA- or $VEGF_{109}$-treated CAMs. *Scale bar*, 25 μm. *HSA*, human serum albumin. *C*, quantitation of lymphangiogenesis from CAM sections. The plot shows the area occupied by lymphatics as a fraction of the total section area. Applied protein amounts are color-coded *blue* (2.5 μg) and *red* (25 μg). *Numbers in parentheses* indicate which VEGF receptors the growth factor binds. The results of the statistical analysis are shown as in Fig. 5. *, **, and *** denote *p* values of <5, 1, and 0.1%, respectively.

sequences. Classical DNA shuffling was not feasible, as the identity between VEGF and VEGF-C is concentrated within the cystine knot; therefore, this method would have caused a strong crossover bias (30). A non-random approach resulted in a library size that allowed exhaustive profiling of the receptor binding pattern of each individual clone. By combining this data with scanning mutagenesis and analysis of receptor deletion mutants, we were able to resolve the VEGF-C binding determinants at three different levels: 1) at the protein domain level of the receptor, 2) at the secondary structure level of the ligand, and 3) at the amino acid residue level of the ligand (summarized in Fig. 7).

Loops 1 and 3 of VEGF-C Contain the VEGFR-3 Specificity Determinants—Large parts of VEGF and VEGF-C were compatible with binding to all receptors. Based on the receptor binding profiles of 398 mosaic molecules, we identified three determinants of VEGFR-3 receptor specificity, two of which are localized in the two loop regions of the cystine knot. VEGF-C-derived fragments 4 and 8 (corresponding to loops 1 and 3) could confer VEGFR-3 binding to VEGF. In similar experiments, VEGF-E-derived loops 1 and 3 conferred VEGFR-2 binding to PlGF, and VEGF-A-derived loops 1 and 3 could functionally replace their counterparts in VEGF-E (31). Such functional replacements required that both loops be derived from the same parent molecule. In contrast to this, the same VEGF-C-derived loops could not functionally replace their VEGF counterparts for VEGFR-2 binding. Together with the fact that VEGF-C binding to VEGFR-2 does not require the presence of the third receptor domain, we conclude that VEGF-C binds VEGFR-2 in a fashion substantially different from VEGF or VEGF-E.

The mutation of seven residues within fragments 4 and 8 into alanine residues resulted in a moderate increase of the K_d for VEGFR-3 between 2 and 8-fold. A more pronounced effect on VEGFR-3 binding was observed for only three mutants, Phe^{151}, Cys^{156}, and Pro^{198}. This suggests the presence of a large binding interface with only few prominent key residues. The homologous residues of Phe^{151} and Pro^{198} in the VEGF- and PlGF-VEGFR-1 complexes directly contact the receptor (4, 5), whereas the homologous cysteine residue is crucial for structural integrity and biological activity (32, 33).

Domain 2 of VEGFR-2 Is Sufficient for VEGF-C Binding, whereas in VEGFR-3, Both Domains 1 and 2 Are Necessary—The bottom regions of VEGF and PlGF may contact the third extracellular Ig homology domain of VEGF receptors, and they have been implicated in receptor binding and specificity (4, 5). Surprisingly, however, the third domain of VEGFR-3 was not required for VEGF-C binding, and instead, the first domain appeared necessary. Given that all VEGFs bind their receptors in a highly similar fashion, it appears unlikely that VEGF-C would interact directly with this domain of VEGFR-3. It has been proposed that domain 1 of VEGFR-1 provides a shield for the hydrophobic surface of domain 2 in the absence of ligand (4). That the first extracellular domain of VEGFR-3 could accomplish such function is supported by the fact that replacement of the first domain of VEGFR-3 by the corresponding domains of platelet-derived growth factor receptor α or colony stimulation factor-1 receptor resulted in the loss of protein secretion,[3] indicating impaired protein folding.

The Role of Subunit Flexibility for Multiple Receptor Binding—In fragment 5, which comprises much of the presumed dimerization interface, 7 of 11 amino acid residues are conserved between VEGF and VEGF-C, most likely because of the constraints imposed by the cystine knot. VEGF-C-derived fragment 5 correlated strongly with VEGFR-3 binding but not with VEGFR-1 binding. In 56 of 67 VEGFR-3 binding mosaic factors, this segment was derived from VEGF-C. The alanine scan of this fragment indicated cysteine 156 as the major important residue within fragment 5. Mutation of this cysteine residue into a serine residue abolished only VEGFR-2 binding (10), whereas mutation to alanine resulted in the loss of binding to both VEGFR-2 and VEGFR-3. For the Cys^{156}→Ala mutant, the ratio of monomeric to dimeric molecules was 4.6 to 1, a similar value as reported for the corresponding Cys→Ser mutation in VEGF, which also abolishes most of the biological activity

[3] M. Jeltsch, and K. Alitalo, unpublished data.

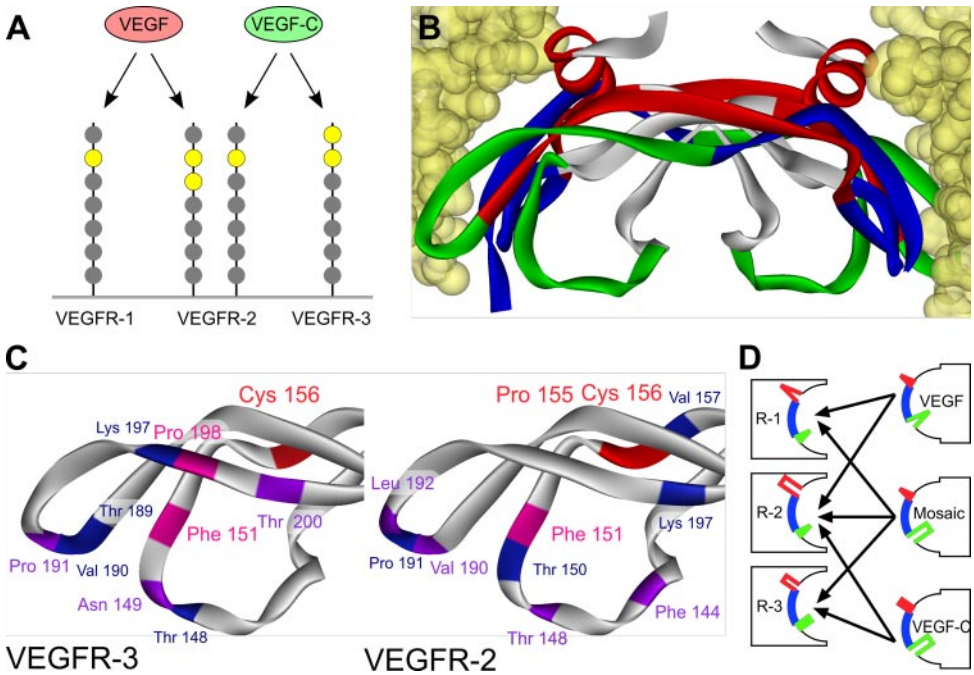

FIGURE 7. **Schematic summary of receptor binding requirements of VEGF *versus* VEGF-C.** *A*, ligand binding domains of VEGF receptors. Domain 2 of VEGFR-1 is sufficient for VEGF binding, whereas in VEGFR-2, both domains 2 and 3 are necessary (4). Domain 2 of VEGFR-2 is sufficient for VEGF-C binding, but in VEGFR-3, both domains 1 and 2 are required. The minimal ligand binding domains are shown in *yellow*. *B*, structural elements for receptor binding of VEGF and VEGF-C shown on a model of VEGF. The VEGF-C regions required and sufficient for VEGFR-3 binding but incompatible with VEGFR-1 binding are shown in *green*. VEGF regions required but not sufficient for VEGFR-1 binding and compatible with VEGFR-3 binding are shown in *red*. The promiscuous part of the receptor binding interface is shown in *blue*, and the van der Waals surface of receptor domain 2 is rendered in *yellow*. *C*, importance of individual amino acid residues from the specificity-determining regions of VEGF-C for VEGFR-2 and VEGFR-3 binding. Indicated are all residues resulting in a >2-fold (VEGFR-3) or 3-fold (VEGFR-2) increase of the apparent K_d when mutated to alanine. The increase of apparent K_d upon mutation to alanine is color-coded red (>20-fold), pink (8–20-fold), violet (4–8-fold), and blue (<4-fold). *D*, schematic illustration of how a mosaic molecule could possibly bind to all three VEGF receptors (*R-1*, *R-2*, and *R-3*). Complementary *shapes* indicate a necessary interaction, whereas non-complementary *shapes* indicate either incompatibility (the *triangular indentation* does not accommodate the *rectangle*) or compatibility (the *rectangular indentation* can accommodate the *triangle*). *Green* represents the bottom face of VEGF/VEGF-C, *red* represents the N-terminal helix of VEGF and the corresponding part of VEGF-C, and *blue* represents binding determinants compatible with all VEGF receptors.

(33). Because the Cys^{156}→Ser mutant also showed a significant monomeric component with a ratio of 2:1, other factors are likely to contribute to the loss of activity of the Cys^{156}→Ala mutation.

Both growth factor ligands of VEGFR-3 are non-covalent dimers (34, 35). Thus, fragment 5 might be involved in rendering the groove between the two subunits of VEGF-C more accessible and/or more flexible than in VEGF, thereby enabling VEGFR-3 binding. However, the non-covalent mode of dimerization does not seem to be directly responsible for the higher accessibility, as several VEGFR-3 binding mosaic molecules were covalent dimers (supplemental data).

The flexibility that allows variable exposure of the bottom groove of VEGF has been implicated in its ability to bind two different receptors (36). However, only the structures of VEGF-VEGFR-2 or VEGF-C-VEGFR-2 and VEGF-C-VEGFR-3 complexes can tell whether the subunit and loop flexibility of VEGFs participate in the receptor specificity determination. The absolute requirement for VEGF-derived fragments 2 and 7 for VEGFR-1 binding and the existence of super-VEGFs support the view that receptor discrimination requires specific structural features separate from an overlapping receptor binding core interface, which might not allow receptor discrimination because of its high conservation. Such structures would include the N-terminal helices of PlGF/VEGF and specific features of the VEGF-C bottom face and would be complemented by specificity-determining structures of the receptors. Because VEGF-derived fragments 2 and 7 did not confer VEGFR-1 binding to VEGF-C (not even in combination with fragment 3), such specificity-determining structures might be accessory and not responsible for the majority of free energy change.

The Specificity-determining Regions of VEGF and VEGF-C Do Not Overlap—Because the specificity-determining structures did not overlap, we were able to create VEGF/VEGF-C mosaic molecules that interact with all three VEGF receptors. We were interested in seeing how such changes in the receptor interaction patterns would translate to biological function. In the CAM assay, which is well suited for the simultaneous evaluation of both the angiogenic and lymphangiogenic potential of growth factors (21, 37, 38), the biological responses toward the VEGF/VEGF-C mosaics were attenuated when compared with equal amounts of the parental molecules. This is not surprising given the library size and the fact that no optimization was performed on the molecules. The relative affinities toward VEGFR-2 and VEGFR-3 were always weaker than those of the parental molecules. Yet, the relative affinity toward VEGFR-1 as well as the potency in the Ba/F3 bioassay appeared unaffected or even slightly increased for some VEGFR-1 binding molecules. This is likely because of the function of the N-terminal helix for VEGFR-1 binding. It carries several VEGFR-1 binding determinants, whereas it is not an integral part of the cystine knot and the associated loops. Therefore, changes in the fine structure of the cystine knot with its loops (which likely comprise more of the binding determinants for VEGFR-2 and VEGFR-3) will have less impact on VEGFR-1 binding than on VEGFR-2 and -3 binding. The weaker biological activity is furthermore explained by the fact that the mosaic molecules contained only the receptor binding domain and no accessory domains. A similar difference in the biological potency between $VEGF_{121}$ and $VEGF_{165}$ has been attributed to the lack of the C-terminal domain in $VEGF_{121}$, which mediates the interaction with neuropilin (39, 40).

The lack of strong lymphangiogenic activity of mosaic 12–11 was unexpected, considering its ability to induce phosphorylation of VEGFR-3. Similarly unexpected was the weak angiogenic response of 84–11, despite its higher potency in activating VEGFR-2 when compared with 12–11, with the latter producing a strong angiogenic response. Whether this difference can be explained by their differential affinity for and activation of VEGFR-1 remains unclear, which highlights our incomplete understanding of the dual decoy *versus* signaling functions of VEGFR-1 in angiogenesis (25, 41, 42). For a few mutants, the changes in affinity, ligand binding, and biological response appeared at least partially uncoupled, something that has been previously described for the ErbB receptor family and its viral ligands (43). A similar mechanism of low level but sustained receptor activation could explain why the Pro^{198}→Ala mutant performed well in the bioassay despite its high K_d.

Angiogenesis or the lack thereof are key events in the development and progression of major pathological conditions, such as tumor growth or ischemic heart disease. Consequently, VEGF-mediated signaling is a major target for therapeutic intervention (44). Recently, it has become clear that VEGF-C also plays a key role in several diseases. Insufficient signaling via VEGFR-3 can be the cause of hereditary lymphedema type I (45), and VEGF-C can promote tumor dissemination via its lymphangiogenic effect (46–49). The mosaic molecules we have described provide a platform for applications that require the fine-tuning of proangiogenic or prolymphangiogenic signaling, whereas knowledge of the receptor interactions of VEGF-C can be utilized to design inhibitors of VEGF-C signaling.

Acknowledgments—We thank Jörg Wilting for invaluable advice on the CAM assay and Tanja Laakkonen for excellent technical assistance.

REFERENCES

1. Clauss, M. (2000) *Semin. Thromb. Hemostasis* **26,** 561–569
2. Carmeliet, P., and Collen, D. (1999) *Curr. Top. Microbiol. Immunol.* **237,** 133–158
3. Ferrara, N. (2001) *Am. J. Physiol.* **280,** C1358–C1366
4. Wiesmann, C., Fuh, G., Christinger, H. W., Eigenbrot, C., Wells, J. A., and de Vos, A. M. (1997) *Cell* **91,** 695–704
5. Christinger, H. W., Fuh, G., de Vos, A. M., and Wiesmann, C. (2004) *J. Biol. Chem.* **279,** 10382–10388
6. Iyer, S., Leonidas, D. D., Swaminathan, G. J., Maglione, D., Battisti, M., Tucci, M., Persico, M. G., and Acharya, K. R. (2001) *J. Biol. Chem.* **276,** 12153–12161
7. Muller, Y. A., Li, B., Christinger, H. W., Wells, J. A., Cunningham, B. C., and de Vos, A. M. (1997) *Proc. Natl. Acad. Sci. U. S. A.* **94,** 7192–7197
8. Li, B., Fuh, G., Meng, G., Xin, X., Gerritsen, M. E., Cunningham, B., and de Vos, A. M. (2000) *J. Biol. Chem.* **275,** 29823–29828
9. Keyt, B. A., Nguyen, H. V., Berleau, L. T., Duarte, C. M., Park, J., Chen, H., and Ferrara, N. (1996) *J. Biol. Chem.* **271,** 5638–5646
10. Joukov, V., Kumar, V., Sorsa, T., Arighi, E., Weich, H., Saksela, O., and Alitalo, K. (1998) *J. Biol. Chem.* **273,** 6599–6602
11. Cunningham, B. C., and Wells, J. A. (1991) *Proc. Natl. Acad. Sci. U. S. A.* **88,** 3407–3411
12. Makinen, T., Jussila, L., Veikkola, T., Karpanen, T., Kettunen, M. I., Pulkkanen, K. J., Kauppinen, R., Jackson, D. G., Kubo, H., Nishikawa, S., Yla-Herttuala, S., and Alitalo, K. (2001) *Nat. Med.* **7,** 199–205
13. Waltenberger, J., Claesson-Welsh, L., Siegbahn, A., Shibuya, M., and Heldin, C. H. (1994) *J. Biol. Chem.* **269,** 26988–26995
14. Pajusola, K., Aprelikova, O., Pelicci, G., Weich, H., Claesson-Welsh, L., and Alitalo, K. (1994) *Oncogene* **9,** 3545–3555
15. Joukov, V., Pajusola, K., Kaipainen, A., Chilov, D., Lahtinen, I., Kukk, E., Saksela, O., Kalkkinen, N., and Alitalo, K. (1996) *EMBO J.* **15,** 290–298
16. Achen, M. G., Jeltsch, M., Kukk, E., Makinen, T., Vitali, A., Wilks, A. F., Alitalo, K., and Stacker, S. A. (1998) *Proc. Natl. Acad. Sci. U. S. A.* **95,** 548–553
17. Achen, M. G., Roufail, S., Domagala, T., Catimel, B., Nice, E. C., Geleick, D. M., Murphy, R., Scott, A. M., Caesar, C., Makinen, T., Alitalo, K., and Stacker, S. A. (2000) *Eur. J. Biochem.* **267,** 2505–2515
18. Makinen, T., Veikkola, T., Mustjoki, S., Karpanen, T., Catimel, B., Nice, E. C., Wise, L., Mercer, A., Kowalski, H., Kerjaschki, D., Stacker, S. A., Achen, M. G., and Alitalo, K. (2001) *EMBO J.* **20,** 4762–4773
19. Stacker, S. A., Vitali, A., Caesar, C., Domagala, T., Groenen, L. C., Nice, E., Achen, M. G., and Wilks, A. F. (1999) *J. Biol. Chem.* **274,** 34884–34892
20. Gerhardt, H., Golding, M., Fruttiger, M., Ruhrberg, C., Lundkvist, A., Abramsson, A., Jeltsch, M., Mitchell, C., Alitalo, K., Shima, D., and Betsholtz, C. (2003) *J. Cell Biol.* **161,** 1163–1177
21. Oh, S. J., Jeltsch, M. M., Birkenhager, R., McCarthy, J. E., Weich, H. A., Christ, B., Alitalo, K., and Wilting, J. (1997) *Dev. Biol.* **188,** 96–109
22. Maragoudakis, M. E., Haralabopoulos, G. C., Tsopanoglou, N. E., and Pipili-Synetos, E. (1995) *Miscrovasc. Res.* **50,** 215–222
23. Abramoff, M. D., Magelhaes, P. J., and Ram, S. J. (2004) *Biophot. Int.* **11,** 36–42
24. Petrova, T. V., Makinen, T., Makela, T. P., Saarela, J., Virtanen, I., Ferrell, R. E., Finegold, D. N., Kerjaschki, D., Yla-Herttuala, S., and Alitalo, K. (2002) *EMBO J.* **21,** 4593–4599
25. Hiratsuka, S., Minowa, O., Kuno, J., Noda, T., and Shibuya, M. (1998) *Proc. Natl. Acad. Sci. U. S. A.* **95,** 9349–9354
26. Shibuya, M. (2001) *Cell Struct. Funct.* **26,** 25–35
27. Olofsson, B., Pajusola, K., von Euler, G., Chilov, D., Alitalo, K., and Eriksson, U. (1996) *J. Biol. Chem.* **271,** 19310–19317
28. Ogawa, S., Oku, A., Sawano, A., Yamaguchi, S., Yazaki, Y., and Shibuya, M. (1998) *J. Biol. Chem.* **273,** 31273–31282
29. Wise, L. M., Veikkola, T., Mercer, A. A., Savory, L. J., Fleming, S. B., Caesar, C., Vitali, A., Makinen, T., Alitalo, K., and Stacker, S. A. (1999) *Proc. Natl. Acad. Sci. U. S. A.* **96,** 3071–3076
30. Joern, J. M., Meinhold, P., and Arnold, F. H. (2002) *J. Mol. Biol.* **316,** 643–656
31. Kiba, A., Naoyuki, Y., and Shibuya, M. (2003) *J. Biol. Chem.* **278,** 13453–13461
32. Muller, Y. A., Heiring, C., Misselwitz, R., Welfle, K., and Welfle, H. (2002) *J. Biol. Chem.* **277,** 43410–43416
33. Potgens, A. J., Lubsen, N. H., van Altena, M. C., Vermeulen, R., Bakker, A., Schoenmakers, J. G., Ruiter, D. J., and de Waal, R. M. (1994) *J. Biol. Chem.* **269,** 32879–32885
34. Joukov, V., Kaipainen, A., Jeltsch, M., Pajusola, K., Olofsson, B., Kumar, V., Eriksson, U., and Alitalo, K. (1997) *J. Cell. Physiol.* **173,** 211–215
35. Stacker, S. A., Stenvers, K., Caesar, C., Vitali, A., Domagala, T., Nice, E., Roufail, S., Simpson, R. J., Moritz, R., Karpanen, T., Alitalo, K., and Achen, M. G. (1999) *J. Biol. Chem.* **274,** 32127–32136
36. Muller, Y. A., Christinger, H. W., Keyt, B. A., and de Vos, A. M. (1997) *Structure* (*Camb.*) **5,** 1325–1338
37. Eichmann, A., Corbel, C., Jaffredo, T., Breant, C., Joukov, V., Kumar, V., Alitalo, K., and le Douarin, N. M. (1998) *Development* (*Camb.*) **125,** 743–752
38. Yamaguchi, S., Iwata, K., and Shibuya, M. (2002) *Biochem. Biophys. Res. Commun.* **291,** 554–559
39. Whitaker, G. B., Limberg, B. J., and Rosenbaum, J. S. (2001) *J. Biol. Chem.* **276,** 25520–25531
40. Keyt, B. A., Berleau, L. T., Nguyen, H. V., Chen, H., Heinsohn, H., Vandlen, R., and Ferrara, N. (1996) *J. Biol. Chem.* **271,** 7788–7795
41. Luttun, A., Tjwa, M., Moons, L., Wu, Y., Angelillo-Scherrer, A., Liao, F., Nagy, J. A., Hooper, A., Priller, J., De Klerck, B., Compernolle, V., Daci, E., Bohlen, P., Dewerchin, M., Herbert, J. M., Fava, R., Matthys, P., Carmeliet, G., Collen, D., Dvorak, H. F., Hicklin, D. J., and Carmeliet, P. (2002) *Nat. Med.* **8,** 831–840
42. Carmeliet, P., Moons, L., Luttun, A., Vincenti, V., Compernolle, V., De Mol, M., Wu, Y., Bono, F., Devy, L., Beck, H., Scholz, D., Acker, T., DiPalma, T., Dewerchin, M., Noel, A., Stalmans, I., Barra, A., Blacher, S., Vandendriessche, T., Ponten, A., Eriksson, U., Plate, K. H., Foidart, J. M., Schaper, W., Charnock-Jones, D. S., Hicklin, D. J., Herbert, J. M., Collen, D., and Persico, M. G. (2001) *Nat. Med.* **7,** 575–583
43. Tzahar, E., Moyer, J. D., Waterman, H., Barbacci, E. G., Bao, J., Levkowitz, G., Shelly, M., Strano, S., Pinkas-Kramarski, R., Pierce, J. H., Andrews, G. C., and Yarden, Y. (1998) *EMBO J.* **17,** 5948–5963
44. Ferrara, N. (2004) *Oncologist* **9,** Suppl. 1, 2–10
45. Karkkainen, M. J., Ferrell, R. E., Lawrence, E. C., Kimak, M. A., Levinson, K. L., McTigue, M. A., Alitalo, K., and Finegold, D. N. (2000) *Nat. Genet.* **25,** 153–159
46. Mandriota, S. J., Jussila, L., Jeltsch, M., Compagni, A., Baetens, D., Prevo, R., Banerji, S., Huarte, J., Montesano, R., Jackson, D. G., Orci, L., Alitalo, K., Christofori, G., and Pepper, M. S. (2001) *EMBO J.* **20,** 672–682
47. Stacker, S. A., Caesar, C., Baldwin, M. E., Thornton, G. E., Williams, R. A., Prevo, R., Jackson, D. G., Nishikawa, S., Kubo, H., and Achen, M. G. (2001) *Nat. Med.* **7,** 186–191
48. Skobe, M., Hawighorst, T., Jackson, D. G., Prevo, R., Janes, L., Velasco, P., Riccardi, L., Alitalo, K., Claffey, K. P., and Detmar, M. (2001) *Nat. Med.* **7,** 151–152
49. Karpanen, T., Egeblad, M., Karkkainen, M. J., Kubo, H., Yla-Herttuala, S., Jaattela, M., and Alitalo, K. (2001) *Cancer Res.* **61,** 1786–1790
50. Veikkola, T., Jussila, L., Makinen, T., Karpanen, T., Jeltsch, M., Petrova, T. V., Kubo, H., Thurston, G., McDonald, D. M., Achen, M. G., Stacker, S. A., and Alitalo, K. (2001) *EMBO J.* **20,** 1223–1231
51. Rodriguez-Niedenfuhr, M., Papoutsi, M., Christ, B., Nicolaides, K. H., von Kaisenberg, C. S., Tomarev, S. I., and Wilting, J. (2001) *Anat. Embryol.* (*Berl.*) **204,** 399–406